



Turbulent and Convective Plasma and its Spatial Structuring Change Drastically the ray Radiative Transfer of Continuous and Discrete (in Lines) Radiation in Internal and External Star Layers

Ostapenko V. A.

Acad. of UAS, Kiev, Ukraine.

Abstract. The problems of the radiation diffusion and the spectral line formation in turbulent-convective plasma are researched on the base of hydrogen plasma of solar active formations. All types of plasma motions such as micro and macro turbulent as well as the directed flows are researched on the background of atom thermal movements. The theory of the spectral line profiles for 3D-structures as the arch systems with intensity plasma flows has been created. The methods of radiation diffusion for homogeneous plasmas earlier need to be reviewed, since the turbulent medium changes the length of free path of photons of radically. The introduction of the average factor of self-absorption enables us to have the efficient way of getting physically correct results.

1. Introduction

Radiative transfer is the physical phenomenon of energy transfer in the form of electromagnetic radiation. The propagation of radiation through a medium is affected by **absorption**, **emission**, and **scattering** processes. The equation of radiative transfer describes these interactions mathematically. Equations of radiative transfer have application in a wide variety of subjects including optics, astrophysics, atmospheric science, and remote sensing. Analytic solutions to the radiative transfer equation (RTE) exist for simple cases but for more realistic media, with complex multiple scattering effects, numerical methods are required.

2. Frequency dependence and radiation transfer in chromosphere plasmas

Frequency dependence of radiation are caused by dissipation or absorption. Optical thickness in a line is usually much higher than the optical thickness in continuous spectrum. Radiation spectrum that passed through such medium of transition zone has absorption lines. Radiation spectrum of optically thin medium has emission lines. If line's optical thickness exceeds one, the intensity of radiation in the center of the line has $\sim B_{\omega}(T)$ and the line will be saturated. As optical thickness further increases, the intensity in the center of the line remains unchanged and its width increases. If optical dense medium has a temperature which drops closer to the surface, the radiation on spectral line frequencies will come out of a cooler part of the medium. In this case, the optical dense of medium (photosphere) radiates of the absorption lines (Ambartsumjan et al., 1952).

$$I(x_n) = I(x_m) e^{-\tau_a(x_{mn})} \quad (1)$$

Full flux attenuation is determined by total optical thickness $\tau_a = \Sigma \tau_{mn}$. A matter between points x_m and x_n is considered to be optically thin at $\tau_a(x_{mn}) \ll 1$ and optically thick at $\tau_a(x_{mn}) > 1$. In general optical thickness depends on radiation frequency ω . If any optically thin region generates its own thermal radiation, its intensity will equal (Conway, 1962):

$$I(\omega) = B_\omega(T) [1 - e^{-\tau_a(x_{mn}, \omega)}], \quad (2)$$

Where $B_\omega(T)$ - emission intensity of absolute black body. If optical thickness of radiation region equals $\tau \gg 1$, the properties of output radiation is determined by external layer with $\tau \sim 1$. In this case, $I(\omega) \sim B_\omega(T)$ with temperature T , which is peculiar for this layer.

A line profile of a homogeneous chromospheres' emission feature, which is located in field of photospheres' emission I_λ^\oplus (Conway, 1962):

$$T(\nu, \tau_{nm}) = S[1 - e^{-\tau_{nm}\alpha(\nu)}] + I_{ph}e^{-\tau_{nm}\alpha(\nu)}, \quad (3)$$

Where $\alpha(\nu) = e^{-\nu}$ is a profile of absorption coefficient for thermal movements of absorbing atoms. The self-absorption factor estimates the number of escaped quanta from optically dense medium.

$$F(\tau_{nm}) = \frac{E(\tau_{nm})}{E(\tau_{nm} = 0)} = \frac{1}{\sqrt{\pi}\tau_{nm}} \int_{-\infty}^{\infty} [1 - e^{-\tau_{nm}\alpha(\nu)}] d\nu. \quad (4)$$

Optical thickness in lines of one spectral series (hydrogen Balmer series) is not independent. They are connected with each other by the ratio (5) through the wavelength λ_{nm} and oscillator force f_{nm} (a number of possible electron states on the quantum level n that allowed by rules of the quantum selection ($\sim 2n^2$)). Optical thicknesses in Balmer lines are related to each other by the ratio

$$(Eljashevich, 1962): \tau_{2m} = \tau_{23} \frac{\lambda_{2m} f_{2m}}{\lambda_{23} f_{23}}. \quad (5)$$

It is illustrated in fig.3d.

Here λ_{nm} is a wavelength for transition from level m to level n , and $S_{nm} = 1 - n^2/m^2$. Oscillator forces f_{nm} for transitions from n to m can be easily calculated by means of gaunt factor g_{nm} :

$$f_{nm} = 1.96028 \frac{ng_{nm}}{m^3 S_{nm}^3}, \quad (6)$$

And probabilities of spontaneous transitions:

$$A_{mn} = f_{nm} \frac{2(1 - S_{nm})}{3\lambda_{nm}^2}, \quad (7)$$

Strengthening (weakening) of spectral line radiation is characterized by the residual intensity value r_ν that is the intensity ratio I_ν to the frequency ν inside the line ($r_\nu = I_\nu/I_\nu^0$). The dependence of residual intensity r_ν on the frequency ν is called a spectral line profile. Full emission (absorption) flux in a unit solid angle on all inside the line frequencies is called full spectral line intensity. The measure that shows part of continuous spectrum is equivalent to full spectral line intensity is called *equivalent width* W_ν of a spectral line.

Active solar processes, primarily solar flares, appear into the absorption lines in the form of radiation reversion (fig.6) and, often, in the form of strips of continuous radiation. The flare appears higher in the chromosphere (model on fig.1a) and usually has higher temperatures than the photosphere. The flare has its own excitation sources, and photospheres' radiation is regarded as external to the flare. Spectral lines of the flare always appear as the emission lines (fig.6).

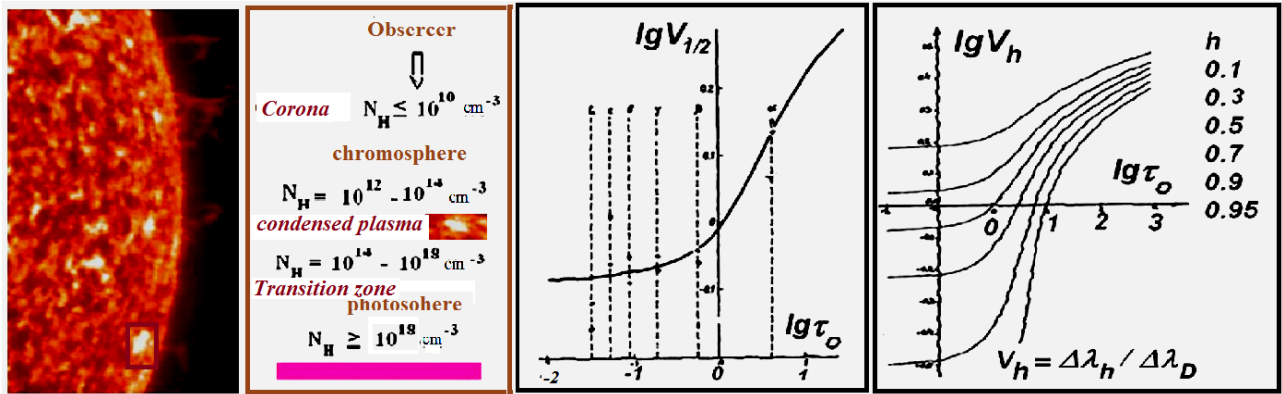


Fig.1. Flare model in solar radiation field. Estimation of optical thickness in Balmer series lines based on observation data in the model of horizontal chromospheres' plasma layer.

- «A fire» in the Sun of 08.03.2009 www.astrogorizont.com.
- The flare model of horizontal chromosphere layer of hydrogen plasma is located above the photosphere.
- «Generalized» *half-width method* of optical thickness determination, which simultaneously takes into account all Balmer hydrogen lines.
- «Generalized» *full-profile method* of optical thickness determination, which simultaneously takes into account the entire profile of all hydrogen lines.

In general case, transfer equation should be used in order to describe a discrete solar flare radiation, which considers all these peculiarities. If we consider a flare source function as constant along the line of sight, then the radiation emerging out of a flare volume is characterized in the size order expression, which is a sum of 1 & 2 expressions. Real flare spectra are deliberately more complicated than those approximations used for their analyses. That's why it is important to consider in detail the reliability of initial assumptions. The choice of an adequate model serves to ensure that received conclusions will be close to the object at least of the order of magnitude. The Sun's photosphere is a very complicated formation, which demonstrates granulation with intense mass plasma streams (fig.2). The photo has finite exposures that have smoothed over real spectra or images. Besides, images provide only a flat layout of solar atmosphere, which in reality is 3D-dimensional. A flat condensed plasma layer located in the chromosphere against the photosphere radiation field (fig.1a) is considered to be a working model of a solar flare. The correlation of all types of flare impulse radiation (radio- 10 cm, optical, UV, X-ray; Shklovsky, 1964) points out to a spatial coincidence (or close location) of generation regions of these emissions.

Examples of flare «cores» and Severny «moustache» line profiles are shown on fig.6 & fig.9. They are characterized by a drop in the center, different deviations from Gaussian function and very lengthened line wings. Moreover, these very broad profiles of «cores» and «moustache» are observed together in space and synchronously in time with completely symmetrical and narrow lines of metals. Fig.8 shows the fragments of solar disk flare spectrum on 15.07.1981. The fragments of 09.07.1982 solar flare spectra show in the region of *MgI 5167.33* & *MgI 5172.68* lines (Ostapenko, 2012). Photometry with the 40-channel MF4A made it first possible to expose the nature of a absorption strips in continuous spectrum. It was our two-dimensional photometry discovered a special status of these continuous spectrum features, as «black» and «white» flares.

3. Macro turbulence and line profiles

The notion of macro-turbulence can be regarded in connection to any object that consists of separate sources of radiation if a statistical number of separate sources fall into a spectral slit.

Another issue is whether we can to apply into such medium the laws of equilibrium distribution of separate source movements in velocities. The presence of spatial structure and directed movements of elements are resulted in the change of object's general view in the spectrum in depending on its distance from the observer. In solar formations these are extensive (*EAS*) and compact (*CAS*) arch systems of active regions. Approaching of observer to object turns *CAS* into *EAS* and vice versa. Such objects cannot be described in the model of stationary equilibrium layers of separate elements. There are three types of movements of radiative atoms. They are thermal movements of separate atoms, micro-turbulent movements of atom' ensembles (plasma remains by laminar and unchanged), and macro-turbulent movements of radiative elements in the volume. Micro-turbulence is taken into account together with thermal movements of atoms. They can be divided by a simultaneous comparison of atoms line profiles, which differ greatly by their atomic weights (hydrogen lines and *H&K CaII*). Macro-turbulence is a mode of homogeneous medium division into movements of separate elements or plasma clusters in time and space.

For a long time the solar atmosphere is considered to be a comparatively homogeneous formation and while using of spectral line profiles thermal and micro-turbulent atoms movements had been considered only. Today both terrestrial and extra-atmospheric observations show an extremely heterogeneous macro structure of solar atmosphere. The surface of the Sun is stormy sea of granules. Their sizes are $\sim 10^3$ km and their lifetime is ~ 10 minutes. As the height gets bigger their fine structure is same visible. The fine details received by Swedish solar vacuum telescope equipped with adaptive optics, which corrects the aberration effects of terrestrial atmosphere.

Profiles of spectral lines in macro-turbulent plasma can be described by a convolution of two functions, which describe the distribution of macroscopic plasma clots (emission elements) movements, thermal and micro-turbulent plasma movements inside every emission element by their velocities (Kurochka & Telnyuk-Adamchuk, 1977, 1978):

$$T(v', \tau_0, \eta) = A \int_{-\infty}^{\infty} [1 - e^{-\tau_0 \alpha(v'-y)}] e^{-(y/\eta)^2} dy, \quad (8)$$

Here $v' = \Delta\lambda / \Delta\lambda_{De}$ - Doppler broadening of emission element line τ_0 - optical thickness of an emission element in the center of a spectral line, $\eta = \Delta\lambda_{Dmac} / \Delta\lambda_{De}$ - the speed velocity ratio of own elements and thermal movements of atoms inside the element. The $\alpha(v')$ - is a profile of spectral line emissivity of one emission element. A coefficient is determined upon normalization condition.

Fig.X shows theoretical profiles (equation 8) of H_α hydrogen and *H&K CaII* lines when applied to active solar formations (prominences & flares; Kurochka et al., 1976). Optical thicknesses of observed *H&K CaII* lines, which are calculated according to Conway equation (homogeneous object), do not exceed several units. Other methods lead to the evaluation of optical thickness in these lines, which equals to about 1000. The assumption of the existence of the macro-turbulent structure, the contradiction has resolved the most natural way. Both the observed and theoretical profiles are confidently itself-agreed between each other. A main consequence of this model is the fact that macro-turbulent plasma movements have a profound influence on spectral lines profiles. Indeed, on fig.4c have modeling the effect on the smoothing on the example of reversing in the center of *H&K CaII* line profile with their specific optical thicknesses. The smoothing effect works so easily that another problem appears. Only smoothing profiles must be observed. In practice, hydrogen and *H&K CaII* lines profiles with intensity reverse in the center and other peculiarities of their transformation are observed. Strong deviations from the Maxwell velocity distribution of emission elements have primarily manifested in lines wings (fig.2c).

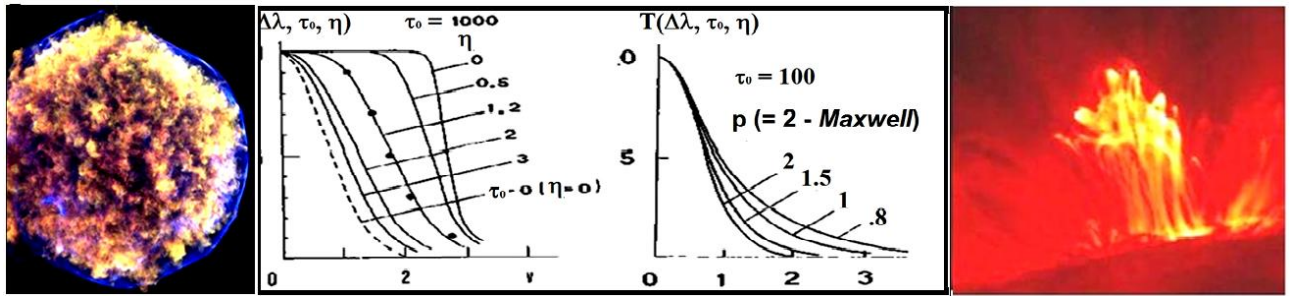


Fig.2. Effects of macro-turbulent plasma structure in spectral line profiles.
(Kurochka & Ostapenko, 1975; Kurochka et al., 1976).

- a. The macro-turbulent radiation source that is the primary stage of the star explosion. APOD 30.04.2011-Tycho' Supernova remnant.
- b. The *K CaII* line profile change for different levels of heterogeneity ($\eta = \Delta\lambda_{Dmac} / \Delta\lambda_{De}$ in formula 8). Dotted line is Gaussian; points are *K CaII* profiles of prominences.
- c. The H_{α} line profile change as the result of the deviation of macro-turbulent velocities distribution from Maxwell distribution.
- d. Macro-turbulent structure of prominences in the Sun's atmosphere.. (NASA NEWS RELEASE, KA TRACE, 16.05.2002).

This fact is important on its own, since the observed line profiles of flare «cores» shown often the extension effect of line wings (fig.2b). Lengthened wings of hydrogen and *H&K CaII* lines in solar flares are the result of plasma stream manifestations. Line profile of macro-turbulent object which is located in the photosphere field of radiation I_{λ}^{\oplus} (Kurochka & Telnyuk-Adamchuk, 1977, 1978):

$$T(v, \tau_0, \eta) = S_e [1 - e^{-\mu(1-F_1)}] + I_{\lambda}^{\oplus} e^{-\mu(1-F_1)}, \text{ and } F_1 = \frac{1}{\eta\sqrt{\pi}} \int_{-\infty}^{\infty} \exp\left[-\frac{\tau_0}{\bar{\mu}} \sqrt{1+\eta^2} e^{-(v+y)^2} - \frac{y^2}{\eta^2}\right] dy. \quad (9)$$

A plasma volume is believed consists of similar emission elements having an optical thickness τ_e and total optical thickness τ_0 , which are related to each by the following ratio:

$$\tau_0 = \frac{\bar{\mu}\tau_e}{\sqrt{1+\eta^2}}. \quad (10)$$

Emission elements are characterized by their own movements which are described by the ratio $\eta = \xi_{mac}/\xi_e$. The velocities distribution of these movements is considered to be a Maxwell distribution. Parameters ξ_{mac} & ξ_e are the most probable velocities of emission element macroscopic movements and thermal movements of atoms inside each element. Parameter $\bar{\mu}$ is an effective number of emission elements along the line of sight. $S_e = const$ is a source function of separate emission element. *The self-absorption factor for macro-turbulent media* we introduced by the next manner. Equivalent width (total energy) of a spectral line is given by the first expression component (9). The $N_m A_{mn}$ quanta appear along the line of sight. The A_{mn} is the probability of $m \rightarrow n$ spontaneous transitions. N_m is the population of upper levels m along the line of sight. So, we obtained:

$$E(\tau_0=0) = N_m A_{mn} h\nu_{mn} = \sqrt{\pi} S_e \tau_0 \sqrt{1+\eta^2}. \quad (11)$$

Then, the self-absorption factor (photons share emitted from the optically dense plasma):

$$F(\tau_0, \eta, \bar{\mu}) = \frac{E(\tau_0)}{E(\tau_0 = 0)} = \frac{1}{\sqrt{\pi} \tau_0 \sqrt{1 + \eta^2}} \int_{-\infty}^{\infty} [1 - e^{-\bar{\mu}(1-F_1)}] dy. \quad (12)$$

When solving the *UST* system of stationary equations, this function determines the number of photons escaping out the object as $N_m A_{mn} F(\tau_0, \eta, \bar{\mu})$. Remaining photons $N_m A_{mn} [1 - F(\tau_0, \eta, \bar{\mu})]$ are absorbed again and excite of plasma by this own radiation field.

With specified optical thickness of the object, self-absorption factor for turbulent plasma $F(\tau_0, \eta, \bar{\mu})$ is always lower than for homogeneous plasma $F(\tau_0)$. For hydrogen in flares $\eta = 0.5-1.0$ (Kurochka et al., 1976) and more $\bar{\mu}$. That's why self-absorption factors for turbulent and uniform medium may be quite different. This enhances the functions of radiative processes in plasma up to the change of calculated physical parameters of emitting plasma.

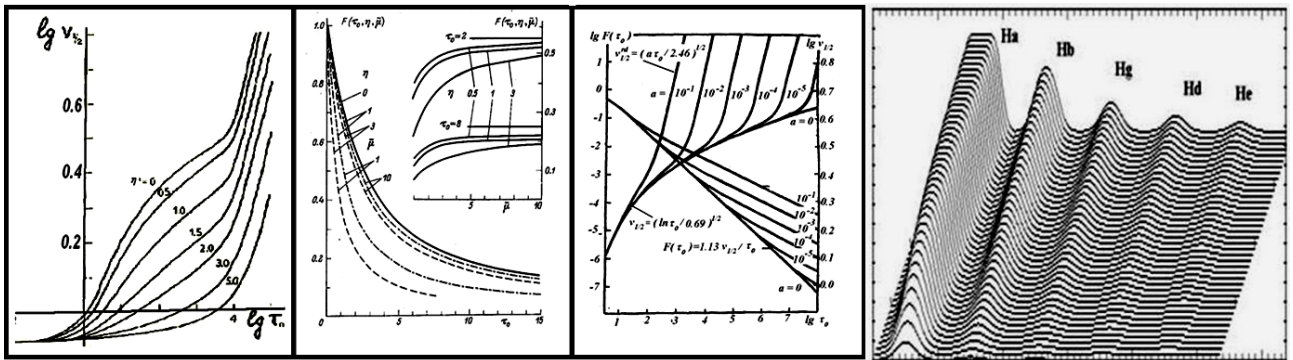


Fig.3. The self-absorption factor $F(\tau_0, \eta, \bar{\mu})$ for homogeneous and heterogeneous emission features.

- a. Turbulent medium (formula 9, Kurochka et al., 1976; Ostapenko, 1981).
- b. Homogeneous medium ($\eta = 0$) for different element overlap $\bar{\mu}$ and $\eta = 0.5, 1, 3$
- c. Homogeneous medium at large optical thicknesses (Kurochka et al., 1975).
- d. The spectral line profiles of the hydrogen Balmer series calculated on the formula 3-7 (in units of $v = \Delta\lambda / \Delta\lambda_D$) and thermal movements of atoms ($T = 9000 K$ and $\tau_{23} =$ from 250 to zero).

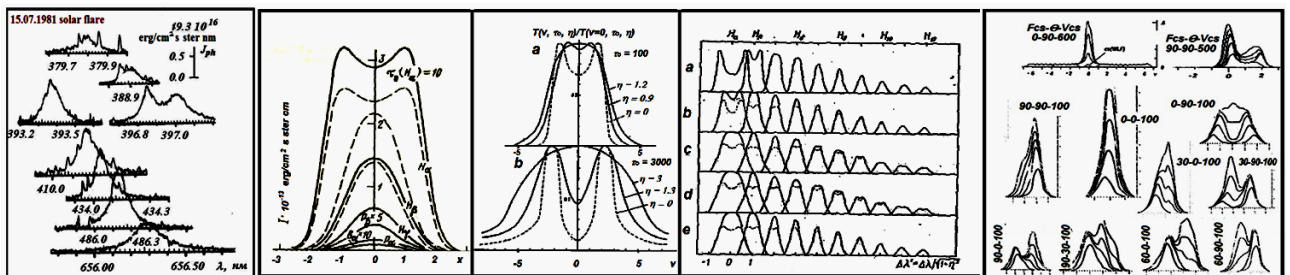


Fig.4. The macro turbulent and stricture influence of different mechanisms resulting in appearance or disappearance of «self-absorption» of spectral lines profiles.

- a. The spectral lines profiles of the hydrogen Balmer series of the 15.07.1981 solar disk flare at the moment of its maximum development (08:18 UT; Leyko & Ostapenko, 1985).
- b. Calculated line profiles (H_{nm}) of solar prominence in the vertical layer model (Yakovkin et al., 1979).
- c. Smearing effect, as the result of macro-turbulence, of H_α ($\tau_0=100$) and $H\&K CaII$ ($\tau_0=3 \cdot 10^3$) «self-absorption» profiles (Kurochka & Ostapenko, 1975).

- d. Calculated view of spectral line profiles of Balmer series due model change (Ostapenko & Zeldina, 1981).
- e. Calculated profiles of point arch systems (PAS) with a current sheet flows for set ($F_{cs} - \theta - V_{cs}$) of places of CS (F_{cs}) in the arch, observer (θ) in its position over the arch and plasma flow velocities (V_{cs}) on the some stages of arisen arch for Severny' "moustache" (fig.7d).

In the fig.4d shows the influence of different mechanisms, which result in the appearance or disappearance of «self-absorption» profiles of Balmer series emission lines (Ostapenko & Zeldina, 1981). The calculations are made by given that $\tau_{23}=100$ and $\Delta\lambda_D/\lambda=0.4 \cdot 10^{-4}$ for different spatial flare models. (a) Variable function of sources ($S \neq const$) for homogeneous ($\eta=0$) model of flat plasma layer. (b) Variable function of sources ($S \neq const$) for inhomogeneous ($\eta=1, \mu<1$) model of horizontal plasma layer. (c) Variable function of sources ($S \neq const$) for inhomogeneous ($\eta=1, \mu<1$) arch model ($\alpha=1.5$) of transparent plasma (there is no mutual screening of arch branches). (d) The same as in clause (c) but at full plasma opacity of front arch branch. (e) Invariable function of sources ($S=const$) for inhomogeneous ($\eta=1, \mu<1$) model of horizontal plasma layer. Profiles calculated for the same models but with the existence of absorption plasma layer over the flare with the following parameters $\tau_{23}=80$ and $\Delta\lambda_D/\lambda=0.3 \cdot 10^{-4}$ are shown in dotted line.

All our modeling have shown that macro-turbulence has a decisive impact on the profiles, easily smoothing all their peculiarities. That's why the possibility of self-absorption appearance in line profiles is very small. It is very important when applying the emission transition while trying to make an exact analysis of processes inside the object (Yakovkin et al., 1979). This mechanism explains the appearance of self-absorption profiles but only in the first among Balmer series lines (fig.4d) as well as the appearance of all described behavior regularities of self-absorption (де Ягер, 1962). Line profiles with «self-absorption» signs in all Balmer series' lines in 16.07.1967 limb flare (Polupan, 1981) are the illustrations to our calculations.

4. Asymmetry and other peculiarities of hydrogen line profiles

Among peculiarities of chromospheres' flares is the existence of so-called *asymmetry* of emission line *profiles*. Hydrogen (H_α) line profiles are usually smooth and symmetrical. But among flares with asymmetric lines profiles about 80% show red asymmetry, where red profile wing is more intense than the blue wing. When approaching closer to the disk edge, red asymmetry decreases and profile width (H_α) increases (Smith & Smith, 1966).

The arch structure of flare emission regions is the key to the asymmetry problem. The information on magnetic field structure is observed both in soft X-ray and extreme ultraviolet, in optics and radio. Magnetic arches are the most typical configurations of objects on the Sun. Each active region consists of discrete, different size loops, filled with plasma (fig.6a & 7c). Observations and show that flares represent the loop systems along filaments (fig.6b). X-ray near-limb images (fig.6a) and limb flares made by NASA's the *TRACE* show bright magnetic loops which plasma. Even young, newly-originated active regions are characterized by a considerable number of small and chaotically distributed loops (Brueckner et al., 1976). Plasma in loops is always moving from the top to both its feet. Magnetic fields are of 600-2500 Gs (Zwaan et al., 1985).

Theoretical line profiles of compact arch formations are researches in the arch model. The aim of this section is calculation of profiles of [hydrogen] lines considering that asymmetry is an outcome of arch structure of radiation region of chromosphere flares and the existence of downward motions of plasma along the arch branches. Let's consider the model (fig.5a) representing the arch of radius R circular cut, which is vertically located in the chromosphere with feet that penetrated into photosphere. Let's consider that emission gets out of a seal layer along the arch branches and moves with angular speed ω . Vector ω has its components (Ostapenko, 1978).

$$\vec{\omega} = \{0, \omega \sin i, \omega \cos i\}. \quad (13)$$

Radiation element with radius-vector $\vec{r} = \{x, y, z\}$ has a velocity components along the line of sight

$$V_z = |[\vec{\omega} \vec{r}]_z| = -x \omega \sin i, \quad (14)$$

And this ray compound results in Doppler shift of wavelength

$$\Delta\lambda/\lambda = V_z/c = -(x \omega \sin i)/c. \quad (15)$$

Doppler shift has a maximum value $\Delta\lambda_{max}$ where $x = R$. So, the probability that Δn of emission elements from n elements has the velocities along the line of sight $V_z \pm \Delta V_z$, then

$$A(v, \alpha) \sim \Delta n/n = \sin \varphi = C \sqrt{1 - (\Delta\lambda / \Delta\lambda_{max})^2} = C \sqrt{1 - v^2 / \alpha^2} \quad (16)$$

The constant C can be calculated from the normalization condition $\int_{-\infty}^{\infty} A(v, \alpha) dv = 1$ and, thus,

$$A(v, \alpha) = \frac{2}{\pi\alpha} \sqrt{1 - \frac{v^2}{\alpha^2}}. \quad (17)$$

$$\Delta\lambda/\Delta\lambda_{max} = x/R = \cos \varphi. \quad (18)$$

Function $A(v, \alpha)$ describes the distribution of line of sight velocities of radiative elements that move in a same direction with a constant angular velocity along the arch. Let's consider that every emission element radiate certain loops $W(v)$ of equal intensity. Lines profiles of a separate radiative element are determined by thermal and micro-turbulent movements of atoms inside the element. Since $W(v)$ and $A(v, \alpha)$ functions describe statistically independent effects, the resulting spectral line profile should have the following formula:

$$T(v, \alpha, \theta) = \int_{y_1(\theta)}^{y_2(\theta)} W(v-y)A(y, \alpha)dy. \quad (19)$$

Variable $v = \Delta\lambda/\Delta\lambda_D$ – line width, $\alpha = \lambda v_0/(c\Delta\lambda_D)$, $v_0 = const$ – plasma flow velocity along the arch branches, $\Delta\lambda_D$ – Doppler width of an emission line of an individual emission element.

Compact formations (sub-flares and cone limb flares) are appeared as arch structures. Let's consider the arch that completely falls into the spectral slit. Let the intensity of the excitation of plasma is the same at all arch points. Suppose that plasma accumulates at the arch top and moves along the arch branches down to arch' foots (Ostapenko, 1978). The $A(v, \alpha)$ function breaks down into four separate zones of integration: I. AB – the zone of a red shift in the interval $\alpha \cos(\theta) \leq v \leq \alpha$; II. BC – the zone of a red shift $\alpha \sin(\theta) \leq v \leq 0$; III. CD – the zone of a blue shift $-\alpha \sin(\theta) \leq v \leq 0$; IV. DE – the zone of a red shift $0 \leq v \leq \alpha \cos(\theta)$. If emission from all arch zones is observed without disturbance, the expression 19 will be written as follows:

$$T(v, \alpha, \theta) = \int_{-\alpha \sin \theta}^{\alpha} W(v-y)A(y, \alpha)dy + \int_{\alpha \sin \theta}^{\alpha} W(v-y)A(y, \alpha)dy. \quad (20)$$

In principle, it may happen that the back branch (zone I, for example) gets weaker or falls completely for the observer due its screening by the face branch. The exclusion of zone I is carried by substituting the first component of equation 20 integration limits α by $\alpha \cos(\theta)$.

It should be remarked that angle of sight (θ), under which the observer looks at the arch, is closely connected with the angle of arch position on the Sun's disk (fig.5c). When θ angle is

reduced to zero (arch is in the center of the disk), zones AB and DE disappear. Zones BC and CD increase to their maximum, while closing to double overlapping of zone $0 \leq v \leq \alpha$. This case corresponds to the biggest red asymmetry. If $\theta \rightarrow \pi/2$ (arch on the limb), zones BC and CD disappear and zones AB and DE are maximum. In this case, the result depends on whether zone I emission reaches the observer. If this emission takes part in the formation of resulting profile, we get a broadened symmetric profile. Otherwise, we get the most probable blue profile asymmetry. Sub-flares are characterized by relatively weak plasma flows. Profiles of thermal movements $W(v)$ prevails here over $A(v, \alpha)$. In this case asymmetry doesn't much perturb the Gaussian profile of thermal plasma movements in emission elements. For study purposes, let's take H_α line profile observed in the solar disk flare on 06.09.1957 as the $W(v)$ profile. This flare was observed in Kiev at Horizontal Solar Telescope (HST-1954). Optical thickness of H_α flare line $\tau_{23} = 80$, Doppler width $\Delta\lambda_D/\lambda = 0.70 \cdot 10^{-4}$ and emission elements' overlapping at the line of sight $\eta = 1$.

Calculations show (fig.5e), that red asymmetry appears at all values $\theta > 50^\circ$ (in accordance with observations; Svestka, 1976). With big angles θ (close to the limb), the orientation of arch plane with regard to the observer becomes quite essential. If the arch returned to the observer its plane (not the edge), the slope angle of the rotation axis (i) decreases (fig.5c), which reduces the parameter α (Ostapenko, 1978)

$$\alpha = \frac{\Delta\lambda_{macro}}{\Delta\lambda_{micro}} = \frac{R\omega}{\Delta\lambda_{micro}} \sin i. \quad (21)$$

Emission elements in arch structures of active region are positioned along the arch branches and move directly from the top down to the basis. If the value of parameter $\alpha \gg 1$, the intensity of directed plasma flows exceeds the intensity of thermal movements.

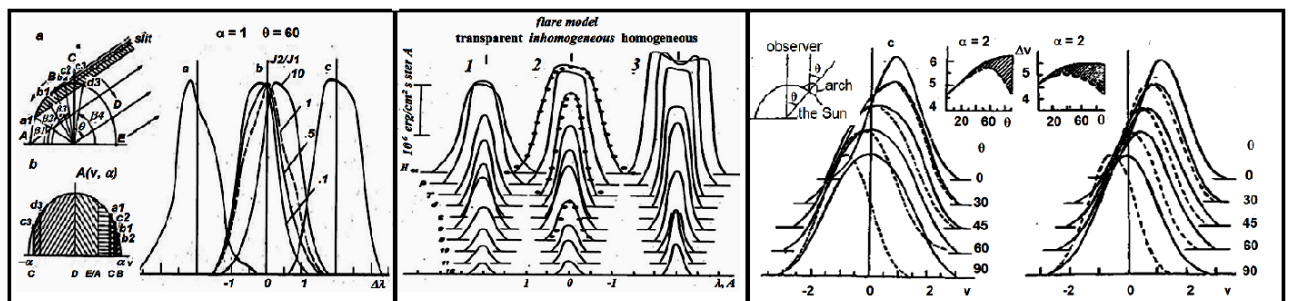


Fig.5. The arch model describes all principal observed statistic regularities of spectral lines profiles of solar flares as well as the appearance of specific flare spectral line features (Ostapenko, 1978).

- | | | |
|---|---|--|
| <p>a. The arch model and spectral line profiles, calculated by formula 19 (in the center) at different intensities of J plasma emission along the arch. Examples of observed profiles: (a) - H_β line (Kazantsev & Polupan, 1979) and (c) - H_α line (Kurochka & Ostapenko, 1970).</p> | <p>b. Change of observed profiles of the 06.09.1957 flare depending on the accepted flare plasma structure (Ostapenko & Kurochka, 1978).</p> | <p>c. The sight angle θ on the arch coincides with the arch position on the Sun's disk. Line profiles (H_α) in the model of compact arch system are calculated by formula .20 with $W(v) = const$.</p> |
|---|---|--|

Function $A(v, \alpha)$ is calculated in $-\alpha < v < \alpha$ range and consists of four separate zones of integration (fig.5). Analysis zones are resulted of the observer's position with regard to the arch (parameters θ and β). Parameter $\beta = 0$ if the arch completely falls into the slit. Parameter β determines the emission point position at the arch and changes starting from zero (the point is situated at the arch basis) and to $\pi/2$, (the point is located at the arch top). This parameter emphasizes any arch zone.

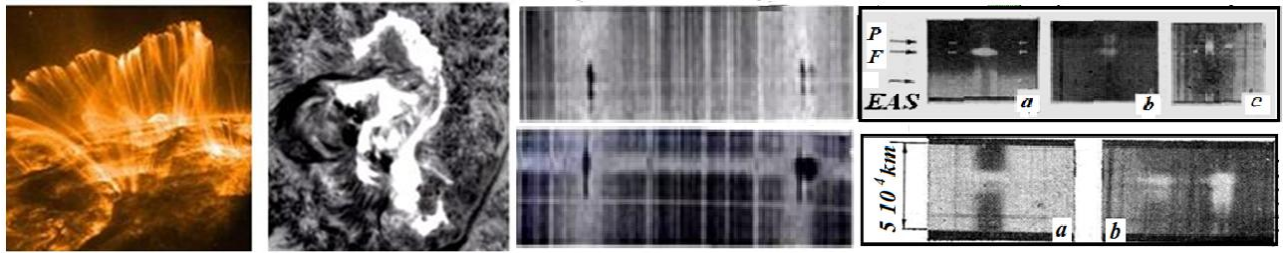


Fig.6. Extended arch systems (EAS) of active regions and their different manifestations on photos in narrow band of spectral lines (left) and in the spectra (right).

- a.** Active region of 09.11.2000 in EUV (side view). The flare produced CME that reached the Earth. (APOD-15.11.2000 - Coronal rain, solar storm- Trace, NASA).
- b.** Powerful flare of 07.08.1972 in H_{α} line (top view of arch arcade; Svestka, 1976).
- c.** Extended arch systems of active region in the flare spectrum 06.09.1957 of a middle powerful (Kurochka & Ostapenko, 1970) and in the spectrum of powerful flare 12.07.1961 (Svestka, 1976).
- d.** The EAS view in $CaII$ lines of the 25.07.1959 limb flare and the disk flares (of the top, Ostapenko et al., 1984). The spectra fragments in the H_{α} (left) & $H_{\epsilon}+H\ CaII$ (of bottom, Nesmjnovich & Ostapenko, 1986).

Let's consider the case shown on fig.5a. An observer looks at the arch at angle of $\sim 60^{\circ}$. Spectrograph's slit cuts a small part of the arch that highlight by fatty line. Total spectral line profile is formed by the following sections of arch branches a_1-b_1 , b_2-c_2 , c_3-d_3 of zones I, II and III, respectively. These sections are highlighted on the fig.5 in bold chain line for the following values $\beta_1=20^{\circ}$, $\beta_2=40^{\circ}$, $\beta_3=\beta_6=80^{\circ}$ and $\beta_4=\beta_5=90^{\circ}$. Function $A(\nu, \alpha)$, which is a part of equation 19, does not equal zero only within limits of these sections. Contours calculation by formula 19 at different emission intensity values of right (zone III and IV) branch to the left (zone I and II) branch (J_2/J_1), are shown on fig.5a (in the middle). Calculations prove that peculiarities of observed profiles can be predetermined by different content of arch branches. We have obtained that macro-turbulence has a decisive impact on the profiles, easily smoothing all their peculiarities. That's why the possibility of self-absorption appearance in line profiles is very small. It is very important when applying the emission transfer while trying to make an exact analysis of processes inside the object (Yakovkin et al., 1979). This mechanism explains the appearance of self-absorption profiles but only in the first among Balmer series lines (fig.4c) as well as the appearance of all described behavior regularities of self-absorption. It is an obvious result of arch structure of flare region.

5. Extend arch systems in spectral lines

Observations show the stability of magnetic field general structure of active region in chromosphere and corona, which is not heavily disturbed even by mid-energetic flares (Ostapenko et al., 1985; Doyle & Widing, 1990). Magnetic arches are by typical configurations of active formations on the Sun and the flare process takes place inside the arcade. *Extended arch systems are seen on chromosphere level of active regions* (fig.6a). The spectrum of a powerful flare on 12.07.1961 (lower fragment is shown on fig.6c) has a strip of suppressed photosphere emission (the «black» BLF flare). Metal emission lines (always narrow) as well as hydrogen emission lines (usually broad) appear (in flares of middle power) only on the background of the continuous emission strip. There are no such strips in weaker flares (06.09.1957 on fig.6c, top fragment). But the most powerful hydrogen and metal lines are visible. It means that current sheet (fig.6d), which manifests as *csBLF* strip, is also present here, but it is a transparent (*csTRF*) feature for photosphere radiation.

Theoretical spectral line profiles of extended arch system (Ostapenko & Palush, 1982). As the flare model (fig.7a) is selected two-dimensional arch, which is cut from arch arcade by the spectral slit. We assume that compressed, in relation to surrounding chromosphere, plasma flows down along arch branches and everywhere has the same excitation degree. Emission of every single area is described by the $W(v)$ single profile, which takes into account only chaotic (thermal and micro-turbulent) plasma motions. The velocities field by plasma flows on an observer line of sight that are placed along the extended arch system branches is described by function $A(v)$. Then the observed spectral line profile is written as the convolution of the A with W :

$$T(v, \alpha, \Theta) = \frac{2}{\pi\alpha} \int_{-\infty}^{\infty} W(v-y)A(y, \alpha, \Theta)dy, \quad (22)$$

Where the multiplier before the integral is found from the normalization condition $\int_{-\infty}^{\infty} A(v, \alpha)dv = 1$

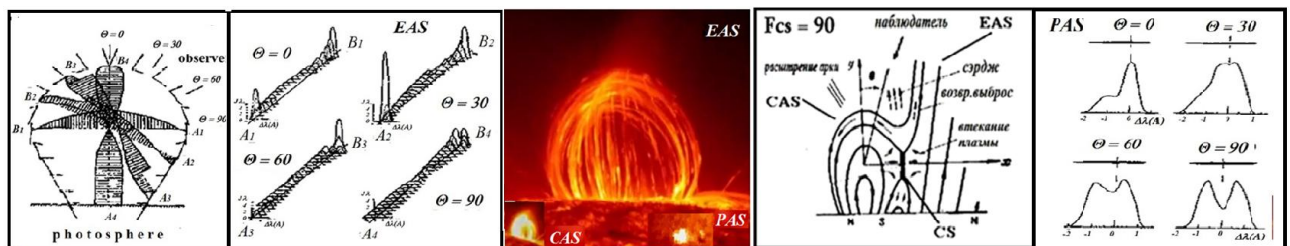


Fig.7. Calculated distribution emission intensity of extend EAS (b) and compact PAS (c) arch systems of active region (Ostapenko, Palush, 1982).

- a. The model of *extend* arch system (EAS), located vertically in the solar chromosphere.
- b. Intensity distribution in spectral line from EAS at different positions of the observer.
- c. Observed Arch Systems on the Sun. APOD-26.02.2013- The rain on the Sun- the SDO, SVS, GSFC, NASA
- d. The model of *compact* (CAS) or *point* (PAS) arch systems with a current sheet (CS).
 - c. Spectral line profiles of *point* arch systems (PAS), calculated in the same EAS model (a).

Profile $T(v, \alpha, \Theta)$ of equation 22 describes arch systems of disappearance small sizes (the $W(v)$ PAS point elements). The profile picture of Extended Arch Systems (EAS) are calculated by means of breaking the function $A(v)$ in equation 22 into separate areas (zones, fig.5a) along arch branches. Let's choose the initial velocity of plasma ejection from the arch top of middle-power flares, which equals to 38 km/s ($\Delta\lambda=0.5 \text{ \AA}$ in *H CaII* line) (Ostapenko & Dolgopolov, 1983). When flowing down, plasma accelerates its movement due to gravitation forces. The author has taken the maximum velocity equal to 150 km/s. Acceleration, for definiteness, is taken as equal to 1.6 km/degree (0.02 $\text{\AA}/\text{degree}$). There are the following plasma flows in arches – towards the observer near the arch apex and away from observer near the base (Georgakilas et al., 1990). We believe that arch itself continuously moves up and keeps both its shape (Rust, 1984) and the pattern of macroscopic plasma motion in arch branches. We will take into account that emission does not get screened when both branches overlap («trans slip light effect»; Ostapenko & Rozhilo, 1985) due the velocity gradient and geometric curvature of the arch. The translucence effect really exists for weak and middle flares as well as on the initial development stage of all flares.

Extensions of line profile wings in CAS or PAS models (fig.7d) are determined by magnetic field strengths, which results the velocity of the current sheet plasma ejection. Velocities (V_{cs}) in some hundred kilometers, partially emerged arch systems, and very extended line profiles are by characters for near-photosphere (PAS; Severny' «usy»). Velocities of one hundred kilometers, entirely emerged arch systems,

and moderately extended line profiles are by characters of chromosphere compact arch systems (*CAS*; *flare «cores»*). A profiles view is resulted by the relative positions of both Observer (θ) and the CS (F_{cs}) to arch

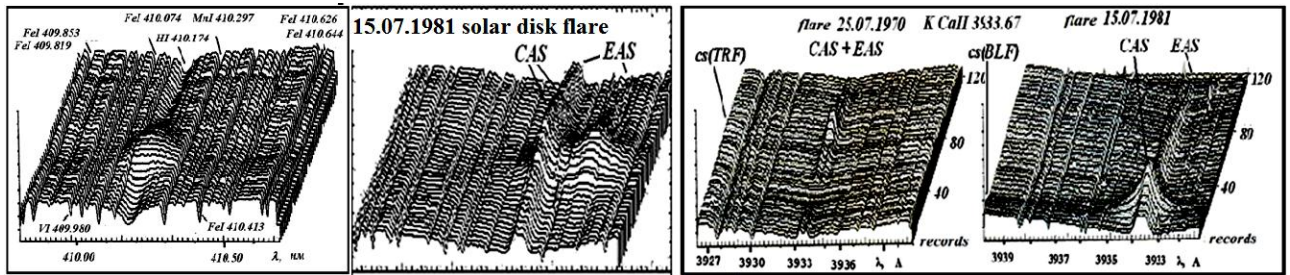


Fig.8. The photometry of the 15.07.1981 solar disk flare spectrum with the 40-channel MF4A that show the view in different spectral lines of extend arch systems (EAS+CAS) of active region (Ostapenko, 2011).

For comparison we give with more dimension the fragments (EAS) of the 25.07.1970 weak flare spectrum (*csTRF*, condensed flare layer does not visible, it is transparent) and our 15.07.1981 powerful flare (EAS (slow component) +CAS «core» or impulse component) around *K CaII* lines.

Note here, if a powerful flare has a core, it also has a *csBLF* (or *csWLF*) strip.

We observe detailed correlation of hydrogen emission lines and *H&K CaII* in chromosphere (Ostapenko, 2011). It gives grounds to expect EAS manifestation in hydrogen lines and strong metal lines. Our MF4A photometry proves this conclusion. Flare emission consists of two components – slow and impulsive. Slow component is a radiation of extend arch systems (EAS) of active region, intensified by a flare. Impulsive component («flare itself») is an emission from a flare core. It's a new magnetic flux CAS, which has extend wings of hydrogen and calcium lines and is always laid on EAS profiles. «Black» flare *csBLF* and emission metal lines on *csBLF* background appear after the origin of extend wings of hydrogen and *H&K CaII* lines.

6. Compact arch systems in spectral lines as the reflect of plasma convection

Active and quiet areas vary on the solar surface. It was the active region numbers (the Wolf numbers) that are by the measure of an activity level of the Sun. At the same time, there are also a set of small centers of activity in undisturbed areas. These are areas of new magnetic fluxes, which are by places of explosive phenomena. These ephemeral (Marsh, 1978) flare-like phenomena (macro-spicules in the H_{α} line) are the same as the *BXP* (Bright X-ray Points) and small bipolar entities on magnetograms. Compact formations are accompanied by surges and they are miniature versions of flares. Most of the *BXP* are not different from the small active regions. Magnetic flux of *BXP* is ~0.2% by magnetic flux of a middle active region (Golub et al., 1979). The *BXP* are placed chaotically across the surface of more than 1000 during the day. This fits with a number (~1375) of EUV- macro spicules. Macro-spicules visible well in H_{α} and D_3 spectral lines both on disk and limb in the form of loops, peaks, nodes. Here we see clear the convective macroturbulence.

The total emission (H_{α}) flare is slow (diffuse) component (H_{α} line width = 2-3 Å) and impulsive component (H_{α} line width = 5-40 Å). The slow component is located on the heights of 5-20 thousand kilometers into arch systems of active regions. Emission of separate (such as Severny «usy» or «moustache») compact sources (H_{α} line width = 5-40 Å) is located at altitudes below 5000 km into arch systems of new magnetic flux. So, the occurrence and development of solar flares fits well with the basic provisions of S. I. Syrovatskij (1976, 1977). In the spectrum (both in optics and UV), it is obviously believed that the flare is the impulsive component (flare «core»). The flare «core» represents a three-dimensional formation with intense plasma flows.

Arch systems of the emerged magnetic flux. Current sheets may and must to form in the collision place of the new emerged compact (CAS) and available extend (EAS) arch systems of active regions. These flare spectra places are flare «cores» (fig.8 & 9).

It is about the very small formations which are emerged near photosphere granules. We put the task to formulate only the basic assumptions of the model. So, the function of $A(v, \alpha)$ in expression 22 we take in simplified its representation in the semicircle form:

$$A(v, \alpha) = \sqrt{1 - \frac{v^2}{\alpha^2}}, \quad (23)$$

Where $v = \Delta\lambda/\Delta\lambda_D$ is the equivalent line width $W(v)$, $\alpha = \Delta\lambda_{max}/\Delta\lambda_D = \lambda v_{dir}/(c \Delta\lambda_D)$, $v_{dir} = \text{const}$ - directional movement velocity of plasma along the arch branches.

Observations indicate that the flaring processes begin immediately after the appearance inside the active region of the new magnetic flux. It was this process that has observed during of our 15.07.1981 flare (Ostapenko, 2011). So, the new arch system can be in process of emerging. The degree of emerging of an arch (fig.5a) is determined by the angular parameter β , which is zero when the arch has been fully floated above the photosphere. And the value of $\beta = 90^\circ$ when the arch is under photosphere entirely. Zones AB, BC, CD, DE (fig.5) represent areas of smooth change of the line of sight velocities. They are not necessarily by a continuous function.

The line profiles of point sources represent in the figure 9. On spectrograms they have the appearance of long narrow strips of discrete radiation, which are located along the dispersion.

The full optical emission of flares consists of mixed emission of impulsive emission of compact formations (velocities of directional movements of plasma is 100-500 km/s) and diffuse emission of extend arch structures (10-100 km/s). The growth of flares power signifies of an increasing of spatial scales of arch systems from 5000 km for sub-flares to 20000 km for the most powerful flares (Mitra et al., 1972). Compact flares are separate new arch structures in active regions of the characteristic sizes of ~5000 km or smaller. The least of them are the «moustache» sources. They have the largest velocities of plasma directional motion (several hundred km/s) and the smallest heights of <1,000 km above the photosphere level. The arch systems have always rooted in their branch basis into photosphere. So, the concept of height (or scale) means the height of the tops of arch systems in chromosphere (or in the corona).

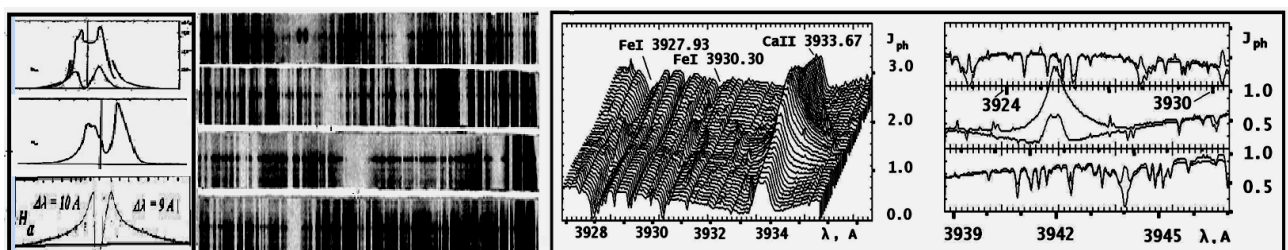


Fig.9. The arch model with the current sheet has written the spectral line profiles of solar flare «cores» (the right panel) as well as the spectral line profiles of Severny' «usy» (Ellerman' «bombs») revealing of the common nature of active solar processes of different scales and powerful (Ostapenko, 2011, 2016).

- a. The most typical profiles of «usy» («moustache»)(Severny, 1957) and
- b. Spectra fragments with continuous emission spectrum of the CS (as «usy») In the *csWLF* stage.

- c. The echelle spectrum MF4A fragment of the 15.07.1981 solar disk flare in range of FeI 3922.92, TiI 3924.53, FeI 3925.91, FeI 3930.30, K CaII 3933.67, AlI 3944.01 lines in the maximal stage of development (08:18 UT). On the right panel the two of 40 photometry records: No.22 (*csBLF* or flare “core”) and No.2 (a spectrum of comparison) (Ostapenko, 2011).

The theory of line profiles for flare «cores» and Severny’s «usy» spectra used the model of turbulent and structuring plasmas allows to write correctly all observed species do not only flares and “Severny” “usy” but and other flare-like events on the Sun. So, the Sun is the entirely by the turbulent plasma. The theory of radiation transfer must to be revised, especially for internal layers of the Sun.

7. Conclusions

The Doppler Effect is of the main mechanism of spectral line profiles extension in solar plasma with magnetic fields. An essential influence on the line profiles is caused by all kinds of movements of atoms. Along with the thermal atom motions, a greatest influence in forming profiles has micro- and macro- turbulence as well as flows of plasma. The turbulence changes the observed line profiles so great that correct values of the optical thickness may be evaluating only by generalized methods that take into account simultaneously all lines of one spectral series. The theory of spectral profiles of turbulent plasma adequate by observations has been created in the Observatory of Kiev T. G. Shevchenko State university in 1970th and is progressed by the author yo the end of 1990th.

Lines profiles of flare «cores» are described in the compact arch model with a current sheet. It is the flare «cores» that are well observed in the spectrum and are the place the interaction of magnetic flows in active region. The together location of the narrow metal lines and the broad hydrogen lines on the background of photosphere darkening strips are confidently explained. The darkening strips (*csBLF* or *csWLF*) are the spectral manifestations of the current sheets in the continuous emission. The broad lines of hydrogen and *H&K CaII* are formed in arch structures of new magnetic flux. The narrow metal lines are formed in *CS* itself.

REFERENCES

- [1] Ambartsumjan V. A., Mustel E. R., Severny A. B., and Sobolev V. V. *Theoretical Astrophysics*. M., “GITTL”, 1952, 635 p. (ru).
- [2] Brueckner G. E., Patterson N. P., Scherrer V. E. *Spectroscopic far ultraviolet observations of transition zone instabilities and their possible role in a preflare energy build-up*. Solar Physics, 1976, v.47, p.127-146.
- [3] Conway M. A. *Theory of Doppler line broadening and self-absorbtion*. Contr. Dun. Obs., 1962, No.3, p.1-5.
- [4] Doyle J. G. & Widing K. G. 1973 *September 7 two-ribbon flare. I. Morphology and loop expansion*. Astrophys. J., 1990, v.352, p.754-759; *II. Physical properties of the loops in the arcade*. Astrophys. J., 1997, v.460, p.760-766.
- [5] Eljashevich M. A. *Atomic and Molecular Spectroscopy*. M., “FM”, 1962, 892 p. (ru).
- [6] Georgakilas A. A., Alissandrakis C. E., Zachariadis Th. G. *Mass motions associated with H_{α} active region arch structures*. Solar Phys., 1990, v.129, p.277-293.
- [7] Golub L., Davis J. M., Krieger A. S. *Anticorrelation of X-ray bright points with sunspot number 1970-1978*. Astrophys. J., 1979, v.229, p.145-150.
- [8] Kazantsev A. M. & Polupan P. N. *Spectra photometry investigations of the 1959-08-18*. Vestnik Kiev. Un-ty. Astronomy, 1979, No.21, p.36-43 (ru).

- [9] Kurochka L. N. & Ostapenko V. A. *Spectra photometry investigations of the 1957-09-06 chromosphere' flare*. Solar Data (Pulkovo), 1970, No.9, p.111-118 (ru).
- [10] Kurochka L. N. & Ostapenko V. A. *Accounting of heterogeneity of objects in the contour line calculations*. Solar data (Pulkovo), 1975, No.7, p.96-102 (ru).
- [11] Kurochka L. N., Ostapenko V. A., Sugay S. P., Palush P. *Contours of emission lines of inhomogeneous solar formations*. Bull. Astron. Inst. Czechosl., 1976, v.27, p.346-353.
- [12] Kurochka L. N. & Telnyuk-Adamchuk V. V. *Line contours of heterogeneous solar entities with various porosities of elements*. Astrometry & Astrophys., 1977, No.33, p.41-51 (ru).
- [13] Kurochka L. N. & Telnyuk-Adamchuk V. V. *Calculation of line profiles of inhomogeneous solar formations/* Solar Phys., 1978, v.59, p.11-19.
- [14] Leyko U. M. & Ostapenko V. A. *Photometry' research of the echelle spectrogram of the 15. VII.1981 solar flare*. Vestnik Kiev. Un-ty. Astronomy, 1985, No.27, p.43-46 (ru).
- [15] Marsh K. A. *Ephemeral region flares and the diffusion of the network*. Preprint BBSO, 1978, No.0175; Solar Phys., 1978, v.59, p.105-113.
- [16] Mitra R. K., Sarkar S. K., Das Gupta M. K. *Some studies on solar optical flares reported under new classification*. Indian. J. Radio and Space Phys., 1972, v.1, p.170-174.
- [17] Ostapenko V. A. *To the question of asymmetry of emission line profiles of chromosphere' flares*. Solar Data (Pulkovo), 1978, No.6, p.80-87; 1978, No.8, p.57-64; 1979, No.4, p.91-96 (ru).
- [18] Ostapenko V. A. & Kurochka L. N. *Photosphere radiation attenuation when it passing through chromosphere' flares*. Solar Data (Pulkovo), 1978, No.11, p.68-75; 1979, No.6, p.87-95 (ru).
- [19] Ostapenko V. A. *Accounting of self-absorption in spectral lines for heterogeneous plasma*. Solar Data (Pulkovo), 1981, No.2, p.90-96 (ru).
- [20] Ostapenko V. A. & Zeldina M. Yu. *About the self-absorption nature of hydrogen spectral line profiles in chromosphere' flares*. Vestnik Kiev. Un-ty. Astronomy, 1981, No.23, p.32-40 (ru).
- [21] Ostapenko V.A., Palush P., *Spectral manifestations of the spatial structure and dynamic processes of chromospheres' flares on the Sun*. Bull. Astron. Inst. Czechosl., 1982, v.33, p.338-345. <http://articles.adsabs.harvard.edu/full/seri/BAICz/0033/0000344.000.html>
- [22] Ostapenko V. A. & Dolgoplov V. I. *Estimation of flow velocity of plasma and magnetic field strength for tops of EAS arch systems on their spectra*. Problems of Space Physics (PKF, Kiev), 1983, No.18, p.24-30 (ru).
- [23] Ostapenko V. A., Yakobchuk A. N., Yarmolenko V. K. *Investigations of the 1959-07-25 limb flare*. Problems of Cosmich. Physics, 1984, No.19, p.25-34 (ru).
- [24] Ostapenko V. A. & Rozhilo A. A. *To the study of conical limb flares*. Vestnik Kiev. University. Astronomy, 1985, No.27, p.46-50 (ru).
- [25] Ostapenko V. A., Palush P., Vatsulik V. *About structure and dynamics of solar flares*. Acta Astronomica et Geophysika Universitatis Comenianaex, 1985, v.10, p.3-25 (ru).
- [26] Ostapenko V.A. *Solar flares: current sheets on the Sun, ecological hydrogen power on the Earth*. Kiev, "Ukraine", 2011, 450 p. (ru); 2012, 185 p. (en).
- [27] Ostapenko V. A. *Research programme of International Geophysical Year (IGY-1957) have ended in the Millennium beginning by discovery of the theoretical current sheets in*

- the Nature*. American Journal of Engineering Research (AJER), 2016, v.5, No.8, p 105-119.
- [28] Polupan P. N. *The spectra photometry of the 16.07.1967 powerful surge' limb flare*. Vestnik Kiev. University. Astronomy, 1981, v.23, p.12-31 (ru).
- [29] Rust D. M. *Permanent changes on filaments near solar flares*. Solar Physics, 1984, v.93, p.73-83.
- [30] Shklovsky I. S. *On the nature of X-ray radiation of the Sun*. Astron. J., 1964, v.41, p.676-683 (ru)
- [31] Smith H. & Smith E. *Solar Flares*. (Ed. A. B. Severny), M., «Mir», 1966, 426 p. (ru).
- [32] Svestka Z. *Solar Flares*. D. Reidel Co., 1976, 400 p.
- [33] Yakovkin N. A., Zeldina M. Yu., Pavlenko Ya. V. *Diffusion of hydrogen radiation in prominences*. Astron. J., 1979, v.56, No.6 (ru).
- [34] Zwaan C., Brants J. J., Cram L. E. *High-resolution spectroscopy of active regions. I. Observing procedures*, Solar Phys., 1985, v.95, p.3-14. *II. Line-profile interpretation, applied to an emerging flux region*, Solar Phys., 1985, v.95, p.15-36.